An extremely low frequency magnetic field and global cerebral ischemia affect pituitary ACTH and TSH cells in gerbils

Snežana Rauš Balind[1], Milica Manojlović-Stojanoski[2], Branka Šošić-Jurjević[2], Vesna Selaković[3], Verica Milošević[2], and Branka Petković[1]

[1]Institute for Biological Research "Siniša Stanković" - National Institute of Republic of Serbia, University of Belgrade, Department of Neurophysiology, Belgrade, Serbia

[2]Institute for Biological Research "Siniša Stanković" - National Institute of Republic of Serbia, University of Belgrade, Department of Cytology, Belgrade, Serbia

[3]Institute for Medical Research, Military Medical Academy (MMA), Medical Faculty MMA, University of Defence, Belgrade, Serbia.

Correspondence to:

Snežana Rauš Balind, PhD

Institute for Biological Research "Siniša Stanković" - National Institute of Republic of Serbia, University of Belgrade, Department of Neurophysiology, Despota Stefana Blvd. 142, 11060 Belgrade, Serbia;

Tel: +381 11 2078 300, fax: +381 11 2761 433;

E-mail: raus.snezana@gmail.com

Running title: ELF-MF and ischemia affect pituitary cells

Conflict of interest: none

Grant sponsors: Ministry of Education, Science, and Technological Development, Republic of Serbia (grant numbers 173009, 173027) and Medical Faculty MMA (MFMMA/11/16-18)

ABSTRACT

The neuroendocrine system can be modulated by a magnetic field and cerebral ischemia as external and internal stressors, respectively. This study deals with the separate or combined effects of an extremely low frequency (ELF) magnetic field (50 Hz, average magnetic field of 0.5 mT) for 7 days and global cerebral ischemia for 10 min on the morpho-functional features of pituitary adrenocorticotrophic (ACTH) and thyrotrophic (TSH) cells in 3-month-old gerbils. To determine the immediate and delayed effects of the applied stressors, measurements were made on the 7^{th} and 14^{th} day after onset of the experiment. The ELF magnetic field and 10-min global cerebral ischemia, separately and particularly in combination, decreased ($p<0.05$) the volume density of ACTH cells, while only in combination was intracellular ACTH content and plasma ACTH concentration increased ($p<0.05$) on day 7. The ELF magnetic field elevated serum TSH concentration on day 7 and intracellular TSHβ content on day 14 ($p<0.05$). Also, 10-min global cerebral ischemia alone increased serum TSH concentration ($p<0.05$), while in combination with the ELF magnetic field it elevated ($p<0.05$) intracellular TSHβ content on day 14. In conclusion, an ELF magnetic field and/or 10-min global cerebral ischemia can induce immediate and delayed stimulation of ACTH and TSH synthesis and secretion.

Keywords: magnetic field; cerebral ischemia; ACTH cells; TSH cells; gerbils

INTRODUCTION

An extremely low frequency (ELF) magnetic field is generated by all electrical devices in our environment. This represents a source of environmental pollution that may induce a variety of effects in organisms. Among them are changes in excitability and synaptic plasticity [Balassa et al., 2013], cell morphology [Rauš Balind et al., 2016], the expression, affinity and density of receptors [Janać et al., 2009; Li et al., 2014], and oxidative stress [Jelenković et al., 2006; Selaković et al., 2013] in the brain, as well as animal behavior [Szemerszky et al., 2010; Janać et al., 2012; Madjid Ansari et al., 2016]. Cerebral ischemia is a pathophysiological condition induced by restricted blood flow through the brain and is a leading cause of death worldwide. It is characterized by a series of events including energy failure, membrane depolarization, increased intracellular Ca^{2+}, massive release of glutamate, greater neuronal excitability, cell damage, oxidative stress, and inflammation [Murdoch and Hall, 1990; Block, 1999; Lewén et al., 2000; Chan, 2001; Doyle et al., 2008; Denes et al., 2010]. Altogether these changes lead to cell death, mainly in the hippocampus or the striatum, which are the most vulnerable brain structures, with consequent altered behavior [Block, 1999]. As potential stressors, both an ELF magnetic field and cerebral ischemia can also affect the neuroendocrine system by acting on the hypothalamus-pituitary-adrenal (HPA) and hypothalamus-pituitary-thyroid (HPT) axes [Rajkovic et al., 2006; Kitaoka et al., 2013; de la Tremblaye et al., 2014; Mahdavi et al., 2014; Radak et al., 2014; O'Keefe et al., 2015; Rauš Balind et al., 2016; Suda et al., 2016].

Stress is a state of disrupted homeostasis that activates the HPA and HPT axes, the two main stress-responsive neuroendocrine systems [Smith and Vale, 2006; Helmreich and Tylee, 2011]. Pituitary adrenocorticotrophic (ACTH) cells provide an essential link between the body and the brain, by controlling adrenocortical glucocorticoid production in response to a sudden or chronic stress. More precisely, afferent inputs from various brain regions (frontal cortex, hippocampus, amygdaloid complex) are summed and integrated in hypothalamic neurons containing corticotropin-releasing hormone (CRH) in the paraventricular nucleus (PVN) [Uchoa et al., 2014]. Hypothalamic CRH further stimulates pituitary ACTH synthesis and

secretion which target the adrenal gland cortex and glucocorticoid output. Glucocorticoids mobilize available energy sources, thus influencing essential physiological functions [Fassbender et al., 1994; Krugers et al., 2000; Zanchi, 2010]. Exposure to various stressors is also associated with thyroid dysfunction [Zhang et al. 2018]. Thyrotropin-releasing hormone (TRH) from the hypothalamic PVN tonically stimulates pituitary thyroid-stimulating hormone (TSH) secretion, which leads to elevated levels of thyroid hormones (TH) in the circulation. TSH cells are essential for HPT axis function, being the feedback set-point that receives stimulatory inputs from neurons, mainly TRH, as well as inhibitory influences from circulating TH. Thus TSH can be considered as the molecule that actually controls metabolic homeostasis, nutritional status, and thermogenesis. Crosstalk between the HPA and HPT axes has been demonstrated and appears to be an adaptive mechanism involved in optimizing energy balance [Haugen, 2009].

The aim of this study was to examine how pituitary ACTH and TSH cells respond to separate or combined influences of an ELF magnetic field (as an external stressor) and global cerebral ischemia (as an internal stressor). The morphometric features of these immunohistochemically/immunofluorescently labeled pituitary cells, i.e. volume density, hormonal output, and storage capacity, were determined in 3-month-old gerbils on days 7 and 14 after onset of the experiment. The animals were exposed to an ELF magnetic field (50 Hz, average magnetic field of 0.5 mT) for 7 days and/or global cerebral ischemia for 10 min. This study is a continuation of previous research [Rauš et al., 2012, 2013; Rauš Balind et al., 2014] and provides further insight into the effects of an ELF magnetic field immediately and one week after cessation of exposure and global cerebral ischemia at different time points after reperfusion. These studies contribute not only in detecting biological effects of the applied ELF magnetic field, as an external stressor, but also in assessing the consequences of such exposure on recovery following global cerebral ischemia in gerbils.

MATERIALS AND METHODS

Animals

The experiments involved 3-month-old male gerbils (*Meriones unguiculatus*, 55-65 g body mass), obtained from the animal facility of the Institute for Medical Research (Military Medical Academy, Belgrade, Serbia). The cages with gerbils (four per cage) were housed in an air-conditioned room at 23 ± 2°C, 55 ± 10% humidity, and with lights on 12 h/day (07:00 – 19:00). The gerbils had free access to commercial food and tap water. All animal procedures were in compliance with Directive 2010/63/EU on the protection of animals used for experimental and other scientific purposes and were approved by the Ethical Committee for the Use of Laboratory Animals of the Institute for Biological Research "Siniša Stanković", University of Belgrade, Serbia.

Experimental Groups

All experiments were performed in a blinded manner. The gerbils were randomly separated into the following groups: (1) Intact – not subjected to a surgical procedure or ELF magnetic field exposure (n = 3); (2) Sham-operated – submitted to the same surgical procedure as ischemic gerbils, but without occlusion of both common carotid arteries (n = 6); (3) Sham-exposed – submitted to the same experimental procedure as ELF magnetic field-exposed gerbils with the electromagnet turned off (n = 6); (4) ELF-MF – continuously exposed to an ELF magnetic field (50 Hz, average magnetic field of 0.5 mT) for 7 days (n = 11); (5) Ischemia – submitted to occlusion of both common carotid arteries for 10 min (n = 11); (6) Ischemia + ELF-MF – submitted to the 10-min occlusion of both common carotid arteries and then exposed to the ELF magnetic field (50 Hz, average magnetic field of 0.5 mT) for 7 days (n = 11).

To evaluate the immediate and delayed effects of the ELF magnetic field and/or 10-min global cerebral ischemia, one half of the animals from each group (except Intact) were sacrificed 7 days and the other half 14 days after onset of the experiment. All parameters were analyzed for each animal separately.

Intact gerbils were in the vivarium for the whole time and were incorporated in the study to exclude any impact of mechanical stress or turned off electromagnet on morpho-functional features of pituitary ACTH and TSH cells. Sham-operated and sham-exposed gerbils were used to evaluate the possible effects of mechanical stress and turned off electromagnet alone, respectively, on the analyzed parameters of ACTH and TSH cells. Preliminary statistical analysis did not show significant differences between and within the control groups (intact, sham-operated, and sham-exposed) for anterior pituitary volume ($F = 0.061$, $df = 4$, $p > 0.05$), the volume density of ACTH cells ($F = 0.220$, $df = 4$, $p > 0.05$), ACTH RIF ($F = 0.257$, $df = 4$, $p > 0.05$), plasma ACTH ($F = 0.365$, $df = 4$, $p > 0.05$), the volume density of TSH cells ($F = 0.063$, $df = 4$, $p > 0.05$), TSHβ RIF ($F = 0.181$, $df = 4$, $p > 0.05$), and serum TSH ($F = 0.542$, $df = 4$, $p > 0.05$). Thus, the effects of the ELF magnetic field and/or 10-min global cerebral ischemia were evaluated in relation to a single control value (presented as a dashed line in the chart) for each of the analyzed parameters.

Global cerebral ischemia

Global cerebral ischemia was achieved by occlusion of both common carotid arteries for 10 min as described in detail in Rauš et al. [2012]. Since gerbils lack collateral communication between the carotid and vertebrobasilar circulation [Levy and Brierley, 1974], they are a good model for inducing global cerebral ischemia.

System for ELF magnetic field exposure

The magnetic field was generated by an electromagnet with a regular laminated transformer core and pole diameter of 9.5 cm. The electromagnet was supplied with a sinusoidal current (50 Hz, 40 V, 4.5 A) producing an ELF magnetic field with a gradient of magnetic induction. Magnetic force lines were parallel to the horizontal component of the local geomagnetic field. Detailed descriptions of the electromagnet and exposure procedure are given in Rauš et al. [2012]. Keeping in mind that the natural electric field strength at power frequencies of 50 or 60 Hz is about 10^{-4} V/m (Environmental Health Criteria of World Health Organization, Geneva (1984)), the effect of the electric field was not considered in this study.

Two cages with gerbils (3-4 per cage) were simultaneously placed one on each side of the electromagnet (Fig. 1A). Their centers were 20 cm far from the electromagnetic poles (Fig. 1B). The gerbils were continuously exposed for 7 days to an average magnetic field (B) of 0.5 mT, measured in the center of each cage. Values of the magnetic field within the cages are shown in Figure 1C. As can be seen, the greatest deviations from the average were observed only in close proximity to the electromagnetic poles. With the electromagnet turned on, temperature changes within the animal cages were slight (up to 0.3°C). To prevent transfer of mechanical vibrations to the animal cages, they were placed at a sufficient distance from the electromagnet to avoid direct contact with it, fixed on foam sponges, and covered with perforated plexiglas plates. The gerbils moved freely within the cages without showing noticeable preferences to stay in any part during the exposure. To avoid the influence of spatial and/or time variation of exposure, the effect of the ELF magnetic field was measured after continuous treatment for 7 days.

Exposure to the ELF magnetic field was performed in an isolated room under identical standard conditions (temperature, humidity, light intensity, and cycle), as in the animal facility where the animals were reared. During the experiment, geomagnetic activity was characterized as “very quiet” (Department of Geomagnetism and Aeronomy, Sector for Geodetic Works, Republic Geodetic Authority, Belgrade, Serbia) measured by a GSM-19 v6.0 proton magnetometer (GEM SYSTEMS, Markham, Canada). Values for the local geomagnetic field (N 44°38', E 20°46') were about 41.8 μT for the vertical component and 22.7 μT for the horizontal component. The background magnetic field did not exceed the value of 10 nT.

Organ processing and immunohistochemistry

The pituitary glands were excised, fixed in Bouin’s solution for 48 h and dehydrated in increasing concentrations of ethanol and xylene. Pituitary sections were stained immunohistochemically (IHC) exactly as previously described [Manojlović-Stojanoski et al., 2012]. Briefly, after the initial tissue deparaffinization, endogenous peroxidase activity was blocked by incubation with 0.3% hydrogen peroxide in methanol for 15 min. Non-specific background staining was reduced by incubation with normal porcine serum (Dako, Copenhagen, Denmark; 1:10) for 45 min. Pituitary ACTH and TSH cells were identified by

incubation with polyclonal rabbit antisera directed against human ACTH (ready to use; Dako, Copenhagen, Denmark) and rat TSHβ subunit (TSHβ; 1:500; A.F. Parlow, National Hormone & Peptide Program, Harbor-UCLA Medical Center, Los Angeles, CA), respectively, overnight at 4°C. Then, the sections were incubated for 1 h with swine anti-rabbit IgG horseradish peroxidase (IgG/HRP 1:100, Dako, Copenhagen, Denmark), applied as the secondary antiserum. Visualizations were performed using diaminobenzidine tetrahydrochloride (DAB; Dako, Copenhagen, Denmark) at concentrations suggested by the manufacturer. The sections were counterstained with hematoxylin and mounted in DPX medium (Sigma-Aldrich, Barcelona, Spain). As a control for nonspecific binding of the secondary antibody, some sections were incubated without the primary antibody. Digital images of immunostained anterior pituitary sections were made with a JVC TK 1280E Video Camera (Leica) on Leica DM RB Photo Microscope (Leica Microsystems, Wetzlar, Germany).

For immunofluorescence, after addition of the primary ACTH or TSHβ antibodies, pituitary sections were incubated with the appropriate immunofluorescent-labeled secondary antibody for 2 h: AlexaFluor 555 donkey anti-mouse IgG for ACTH (Invitrogen Life Technologies, Carlsbad, CA) or AlexaFluor 555 donkey anti-rabbit for TSHβ (Invitrogen Life Technologies, Carlsbad, CA). The sections were then cover-slipped with Mowiol 488 (Sigma-Aldrich, St. Louis, MO). Images were obtained using a confocal laser scanning microscope Leica TCS SP5 II Basic (Leica Microsystems, Wetzlar, Germany). An Arion 555-nm laser was used for excitation of fluorescence.

Stereological measurements

Stereological analysis was performed on a workstation comprising a microscope (Olympus, BX-51, Hamburg, Germany) equipped with a microcator Heidenhain MT1201 (Heidenhain, Traunreut, Germany) to control movements in the z–direction (0.2 μm accuracy), a motorized stage (Prior) for stepwise displacement in x–y directions (1 μm accuracy), and a CCD video camera Pixelink (Pixelink, Ottawa, Canada). The whole system was controlled by the newCAST stereological software package (VIS – Visiopharm Integrator System, ver. 2.12.1.0, Visiopharm, Copenhagen, Denmark). The main objectives used were planachromatic

10x and 20x dry lenses. Control of stage movements and interactive test grids (uniformly spaced points test grids and rectangular unbiased dissector frames) were provided by newCAST software.

Volume estimation of the anterior pituitary

Anterior pituitary volume was determined using Cavalieri's principle [Gundersen and Jensen, 1987], as an unbiased way of estimating the volume of an object by dividing it into a series of parallel planes with a known distance between them. The total volume of the object was determined by summing the areas over all sections and multiplying the results by the section thickness. Mean section thickness was estimated using the block advance (BA) method [Dorph-Petersen et al., 2001]. Every 40th section from each tissue block was analyzed. All points falling within the boundaries of the anterior pituitary were counted and the areas calculated. The volume (mm^3) of the anterior pituitary was obtained by multiplying the sum of the areas by the interval between the sections (200 μm), according to the formula:

$$V_{faze} = a(p) \cdot BA \cdot \sum_{i=1}^{n} Pi$$

where a(p) is the area associated with each sampling point (8355.15 μm^2); BA, the block advance, is the mean distance between two consecutively studied sections; n is the number of sections studied for each pituitary; and ΣPi is the sum of points hitting a given target.

Volume density of pituitary ACTH and TSH cells

The percentage of ACTH and TSH cells per unit volume of the anterior pituitary, i.e. the volume density, is equivalent to the total volume occupied by ACTH and TSH cells divided by the volume of the anterior pituitary and multiplied by 100. The test grid generated by the new CAST software is characterized by uniformly spaced test points for histomorphometric assessment. Test points hitting the immunohistochemically stained ACTH and TSH cells (Pp) were divided by the number of points hitting the reference space (Pt), i.e. the analyzed pituitary section:

$$V_V (\%) = Pp / Pt \times 100.$$

The volume density was calculated for each animal and then expressed as the average value per group.

Relative intensity of immunofluorescence (RIF)

To assess intracellular hormonal content in the pituitary, the relative intensity of immunofluorescence (RIF) in the cytoplasm of ACTH and TSH cells was evaluated exactly as previously reported [Manojlović-Stojanoski et al., 2016]. Fluorescence microscope images were analyzed using Image J software [Jensen, 2013]. In brief, ACTH and TSH cells were encircled with the drawing/selection tool. Their immunonegative nuclei, together with two different immunonegative spots in close proximity to the immunopositive cells, served as reference particles for definition of background fluorescence. RIF was calculated as an average value measured for immunopositive cells subtracted by the average for background fluorescence. The intensity of fluorescence was determined in 100 pituitary ACTH and TSH cells per animal, in which cell nuclei were visible. The sections were examined and photographed using a Zeiss Axiovert fluorescence microscope, equipped with a camera and EC Plan-Apochromat (Carl Zeiss, Jena, Germany).

Hormonal analyses

Plasma ACTH concentration was determined with the COBAS e-411 kit (Roche Diagnostics, Mannheim, Germany) in duplicate samples within a single assay. The intra-assay coefficient of variation (CV) was 1.5-5.4% and analytical sensitivity was 1 pg/ml.

Serum TSH concentration was determined on an IMMULITE automatic analyzer (DPC, Los Angeles, CA), in duplicate samples within a single assay. The intra-assay CV was 4.5-12.5% and analytical sensitivity was 6.4 μlU/ml.

Data presentation and statistical analysis

The results are expressed as means ± SEM. Before statistical analysis, normal distribution of the data was assessed using the Kolmogorov–Smirnov test. If the values did not fit a normal distribution, logarithmic transformation was applied prior to analysis. One-way analysis of variance (ANOVA) was performed to

detect significant differences between groups. When appropriate, subsequent comparisons were made by the Least Significant Difference (LSD) test. The probability $P < 0.05$ was considered as a significant difference.

RESULTS

Anterior pituitary volume

No significant differences ($F = 1.723$, $df = 6$, $p > 0.05$) between any experimental groups were found for the volume of the anterior pituitary (Fig. 2).

Effects of exposure to the ELF magnetic field and/or global cerebral ischemia for 10 min on ACTH cells

Histological examination

ACTH cells were numerous, evenly distributed throughout the anterior pituitary *pars distalis* of control animals, with intense cytoplasmic immunohistochemical staining (Fig. 3A). With prominent nuclei they were oval or polygonal in shape, with cytoplasmic processes extended around and between neighboring cells. In the ELF-MF, Ischemia, and Ischemia + ELF-MF groups fewer ACTH cells were present, while the intensity of immunohistochemical staining varied from pale to dark on day 7 (Fig. 3B, D, F). The morphology and distribution of ACTH cells in these groups regained the control appearance on day 14 (Fig. 3C, E, G).

In line with the immunohistochemical observations, analysis of cytoplasmic immunofluorescence on day 7 revealed fewer ACTH cells in the ELF-MF, Ischemia, and Ischemia + ELF-MF groups, particularly in the last, (Fig. 4B, D, F) when compared to the Control group values (Fig. 4A). The observed changes in ACTH cell number and appearance in these groups returned to the control level by day 14 (Fig. 4C, E, G).

Morphometric measurements

Morphometric measurements confirmed the histological observations (Fig. 3H). Separate or combined exposure to both stressors affected the volume density of ACTH cells ($F = 8.490$, $df = 6$, $p < 0.001$).

Compared to Control group values, the volume density of ACTH cells was significantly lower after exposure to the ELF magnetic field and 10-min global cerebral ischemia by 23% and 25% ($p < 0.05$), respectively, on day 7 (Fig. 3H). At the same time point the observed decrease compared to the Control group was greater (36%; $p < 0.001$) for the Ischemia + ELF-MF group.

There were no significant differences between the Control group and the ELF-MF, Ischemia, and Ischemia + ELF-MF groups for volume density of ACTH cells on the 14^{th} day (Fig. 3H). However, volume density of ACTH cells in the Ischemia group was significantly greater ($p < 0.01$) than in the ELF-MF group.

Comparison of the volume density of ACTH cells on days 7 and 14 revealed marked increases ($p < 0.001$) in the Ischemia and Ischemia + ELF-MF groups on the 14^{th} day (Fig. 3H).

RIF signal and plasma ACTH concentration

The ACTH RIF values ($F = 2.667$, $df = 6$, $p < 0.05$) and plasma ACTH concentrations ($F = 2.567$, $df = 6$, $p < 0.05$) were affected by separate or combined exposure to the two stressors.

The intensity of ACTH fluorescence was enhanced by as much as 90% ($p < 0.05$) in the Ischemia + ELF-MF group on day 7 compared to Control group fluorescence intensity (Fig. 4H), while plasma ACTH concentration was 40% higher ($p < 0.05$) than for the Control group at the same time point (Fig. 5).

On the day 14 no statistically significant differences between the Control group and the ELF-MF, Ischemia, and Ischemia + ELF-MF groups were observed for either intensity of ACTH fluorescence (Fig. 4H) or plasma ACTH concentration (Figs. 5). However, both parameters were significantly higher ($p < 0.05$ and $p < 0.01$, respectively) in the Ischemia + ELF-MF group than in the Ischemia group. Moreover, plasma ACTH concentration was higher ($p < 0.05$) in the ELF-MF group compared to the Ischemia group.

Comparison of values for plasma ACTH concentration obtained on days 7 and 14 revealed a significant decline ($p < 0.05$) in the Ischemia group on day 14 (Fig. 5).

Effects of exposure to the ELF magnetic field and/or global cerebral ischemia for 10 min on TSH cells

Histological examination

Polygonal or oval TSH cells were mainly localized in the medioventral portion of the anterior pituitary *pars distalis* in small groups or as single cells, often in close proximity to capillary vessels (Fig. 6A-G). A granular, intense immunofluorescencent signal for TSHβ was present in the cytoplasm of the cells, which had prominent, often eccentrically located nuclei in all experimental groups (Fig. 6A-G and 7A-G).

Morphometric measurements

Separate or combined exposure to the ELF magnetic field and global cerebral ischemia for 10 min had no effect on the volume density of pituitary TSH cells ($F = 0.939$, $df = 6$, $p > 0.05$). This parameter remained unchanged at both analyzed time points on days 7 and 14 (Fig. 6H).

RIF signal and serum TSH concentration

One-way ANOVA of the TSHβ RIF signal ($F = 2.990$, $df = 6$, $p < 0.05$) and serum TSH concentration ($F = 4.225$, $df = 6$, $p < 0.01$) revealed significant effects of separate or combined exposure to the ELF magnetic field and global cerebral ischemia for 10 min.

TSHβ RIF was markedly increased by 125% in the ELF-MF group ($p < 0.01$) and by 112% in the Ischemia + ELF-MF group ($p < 0.05$) on day 14, in comparison with the Control group (Fig. 7H). Also, it was significantly greater ($p < 0.05$) in the ELF-MF and Ischemia + ELF-MF groups compared to the Ischemia group.

Comparison of values for TSHβ RIF obtained on the 7^{th} and 14^{th} day revealed a significant increase ($p < 0.05$) in the ELF-MF group on day 14 (Fig. 7H).

A significantly elevated serum TSH concentration (by 102%; $p < 0.01$) was detected in the ELF-MF group on day 7 but the value had returned to the control level on day 14 (Fig. 8). The observed increase on day 7 was also significant ($p < 0.05$) when compared to the Ischemia group value.

In the Ischemia group, serum TSH concentration was 78% higher ($p < 0.05$) than for the Control group on day 14 (Fig. 8). This increase was also statistically significant ($p < 0.01$) in comparison with the Ischemia + ELF-MF group.

Serum TSH concentrations decreased significantly between days 7 and 14 in the ELF-MF ($p < 0.01$) and Ischemia + ELF-MF groups ($p < 0.05$) (Fig. 8).

DISCUSSION

The results of this study revealed that separate or combined exposure to an ELF magnetic field (50 Hz, average magnetic field of 0.5 mT) for 7 days and global cerebral ischemia for 10 min affected some morpho-functional features of pituitary ACTH and TSH cells in gerbils. Both stressors, separately and particularly in combination, induced immediate stimulation of ACTH synthesis and secretion. The stimulatory effect of the ELF magnetic field on TSH cells was immediate and persisted for 7 days after cessation of exposure. Also, 10-min global cerebral ischemia alone and in combination with the ELF magnetic field enhanced secretion and synthesis of TSH. This effect was delayed and somewhat attenuated by exposure to the magnetic field.

Exposure to the ELF magnetic field decreased the volume density of ACTH cells, while intracellular ACTH content and plasma ACTH concentration increased slightly but not significantly. These results may be explained by greater release of ACTH into the circulation 7 days after onset of the experiment. This is supported by our earlier findings that rat ACTH cells recognize and respond to short-term (1 and 7 days) and long-term exposure (from conception to 3 months of age) to an ELF magnetic field with the same characteristics as in the current study [Rauš Balind et al., 2016]. The immediate effects of a 1-day exposure to the ELF magnetic field were the most prominent, concerning decreases in the number and size of ACTH cells and their nuclei [Rauš Balind et al., 2016]. Published data related to such effects on circulating ACTH and cortisol/corticosterone levels are not consistent and different modes of ELF magnetic field treatments increased or failed to evoke changes in hormone concentrations [Selmaoui et al., 1997; Sert et al., 1999; Szemerszky et al., 2010; Touitou and Selmaoui, 2012; Kitaoka et al., 2013; Mahdavi et al., 2014]. These contradictory findings point to the complexity and unpredictability of the biological effects of an ELF

magnetic field and could be explained by its peculiarities (frequency, magnetic induction, exposure duration) and the organism studied (species, age, sex).

In ischemic gerbils the significant decrease of the volume density of ACTH cells, together with raised circulating ACTH as a result of secretion was observed on day 7. Most probably this was due to altered negative feedback regulation of the HPA axis, as marked changes in higher regulatory centers including the hippocampus and hypothalamic PVN were established following ischemia [de la Tremblaye et al., 2014]. Namely, reduction of neurons positive for glucocorticoid receptors at the hippocampal CA1 subfield and significant elevation of CRH and its receptor at the PVN in ischemic rats [de la Tremblaye et al., 2014] are in line with the data presented here. These authors also showed elevated corticosterone levels in rats on day 7 of reperfusion that returned to the control level by day 14 of reperfusion. Altogether, these findings indicate that the time after start of reperfusion has a major impact on HPA axis activity.

Immediate effects of the combined stressors were a significant decrease of the volume density of ACTH cells, increased intracellular ACTH content, and raised plasma ACTH concentration. The obtained results indicated that both ACTH synthesis and hormone secretion were intensified, as described earlier [Rauš et al., 2013; Rauš Balind et al., 2016]. The influence of both stressors on ACTH cells 7 days after onset of the experiment had subsided to the control level by day 14.

The impact of the ELF magnetic field on pituitary TSH cells was detected immediately on day 7 after onset of the experiment as an increased concentration of serum TSH, while a delayed effect was recognized on day 14 as elevated intracellular TSH content. These results indicate intensified secretion and synthesis of this glycoprotein hormone in the anterior pituitary in relation to this treatment. TSH is a major tonic regulator of thyroid growth and function. In line with our findings and based on light microscopic and ultrastructural data in rats, Rajkovic et al. [2006] demonstrated stimulation of the thyroid gland by a power-frequency electromagnetic field (EMF; 50 Hz, 100-300 μT, 54-160 V m^{-1}) immediately after exposure. The degree of structural changes in the thyroid correlated well with the duration of exposure, as activity decreased in rats exposed to the EMF for a longer period of time [Matavulj et al., 1999; Rajkovic et al.,

2003]. In contrast to our results, changes in serum TSH and thyroid hormone concentrations were not observed in rats exposed to a 50 Hz sinusoidal magnetic field of 0.75 mT for 3 h/day during one month [Sert et al., 1999] and humans acutely exposed to either continuous or intermittent 50 Hz linearly polarized magnetic fields of 10 μT [Selmaoui et al., 1997].

In the present study, global cerebral ischemia for 10 min did not alter serum TSH concentration immediately, but elevated serum TSH was measured on day 14 after onset of the experiment. In parallel, somewhat increased volume density of pituitary TSH cells was detected in the gerbil model. This effect may be explained by the time needed to re-establish neuro-endocrine control after ischemia. Published data suggest that a low free triiodothyronine (fT_3) level is associated with poor post-stroke functional outcomes 3 months after acute ischemia in stroke patients, while complex causality between TSH level and stroke recovery merits further investigation [O'Keefe et al., 2015; Suda et al., 2016]. The results obtained from *in vitro* studies indicate a protective role of T_3 against glutamate toxicity in neurons and glial cells [Losi et al., 2008; Mendes-de-Aguiar et al., 2008]. Therefore, low fT_3 may negatively affect neuroprotection, leading to increased secondary damage after ischemic stroke. Determination of circulating and local brain thyroid hormone concentrations in our model are needed to evaluate this possibility.

Combined exposure to both stressors intensified intracellular TSH content, while serum TSH concentration remained unchanged on the 14^{th} day after onset of the experiment. Keeping in mind that serum TSH concentration was increased on day 14 in gerbils submitted to 10-min global cerebral ischemia alone, it seems logical to assume that exposure to the ELF magnetic field partly neutralized the effect of global cerebral ischemia.

In conclusion, these findings contribute to the relatively limited pool of results regarding the effects of ELF magnetic fields on pituitary hormone production and secretion in the gerbil model of global cerebral ischemia. Therefore, they may be of importance in assessing the consequences of such exposure on recovery following global cerebral ischemia and even more may be of clinical relevance related to decisions about applying magnetic fields for treating people who had suffered stroke. The potential limitation of this study is

the lack of data about the influence of the two stressors, individually and in combination, on circulating levels of hypothalamic CRH and TRH, corticosterone and thyroid hormones. These data would provide more complete insight into the state of the HPA and HPT axes after exposure to these stressors.

REFERENCES

Balassa T, Varró P, Elek S, Drozdovszky O, Szemerszky R, Világi I, Bárdos G. 2013. Changes in synaptic efficacy in rat brain slices following extremely low-frequency magnetic field exposure at embryonic and early postnatal age. Int J Dev Neurosci 31:724-730.

Block F. 1999. Global ischemia and behavioural deficits. Prog Neurobiol 58:279-295.

Chan PH. 2001. Reactive oxygen radicals in signaling and damage in the ischemic brain. J Cereb Blood Flow Metab 21:2-14.

de la Tremblaye PB, Raymond J, Milot MR, Merali Z, Plamondon H. 2014. Evidence of lasting dysregulation of neuroendocrine and HPA axis function following global cerebral ischemia in male rats and the effect of Antalarmin on plasma corticosterone level. Horm Behav 65:273-284.

Denes A, Thornton P, Rothwell NJ, Allan SM. 2010. Inflammation and brain injury: acute cerebral ischaemia, peripheral and central inflammation. Brain Behav Immun 24:708-723.

Dorph-Petersen KA, Nyengaard JR, Gundersen HJ. 2001. Tissue shrinkage and unbiased stereological estimation of particle number and size. J Microsc 204:232-246.

Doyle KP, Simon RP, Stenzel-Poore MP. 2008. Mechanisms of ischemic brain damage. Neuropharmacology 55:310-318.

Fassbender K, Schmidt R, Mössner R, Daffertshofer M, Hennerici M. 1994. Pattern of activation of the hypothalamic-pituitary-adrenal axis in acute stroke. Relation to acute confusional state, extent of brain damage, and clinical outcome. Stroke 25:1105-1108.

Gundersen HJ, Jensen EB. 1987. The efficiency of systematic sampling in stereology and its prediction. J Microsc 147:229-263.

Haugen BR. 2009. Drugs that suppress TSH or cause central hypothyroidism. Best Pract Res Clin Endocrinol Metab 23:793-800.

Helmreich DL, Tylee D. 2011. Thyroid hormone regulation by stress and behavioral differences in adult male rats. Horm Behav 60:284-291.

Janać B, Selaković V, Rauš S, Radenović L, Zrnić M, Prolić Z. 2012. Temporal patterns of extremely low frequency magnetic field-induced motor behavior changes in Mongolian gerbils of different age. Int J Radiat Biol 88:359-366.

Janać B, Tovilović G, Tomić M, Prolić Z, Radenović L. 2009. Effect of continuous exposure to alternating magnetic field (50 Hz, 0.5 mT) on serotonin and dopamine receptors activity in rat brain. Gen Physiol Biophys 28:41-46.

Jelenković A, Janać B, Pešić V, Jovanović DM, Vasiljević I, Prolić Z. 2006. Effects of extremely low-frequency magnetic field in the brain of rats. Brain Res Bull 68:355-360.

Jensen EC. 2013. Quantitative analysis of histological staining and fluorescence using ImageJ. Anat Rec (Hoboken) 296:378-381.

Kitaoka K, Kitamura M, Aoi S, Shimizu N, Yoshizaki K. 2013. Chronic exposure to an extremely low-frequency magnetic field induces depression-like behavior and corticosterone secretion without enhancement of the hypothalamic-pituitary-adrenal axis in mice. Bioelectromagnetics 34:43-51.

Krugers HJ, Maslam S, Korf J, Joëls M, Holsboer F. 2000. The corticosterone synthesis inhibitor metyrapone prevents hypoxia/ischemia-induced loss of synaptic function in the rat hippocampus. Stroke 31:1162-1172.

Levy D, Brierley J. 1974. Communications between vertebro-basilar and carotid arterial circulations in the gerbil. Exp Neurol 45:503-508.

Lewén A, Matz P, Chan PH. 2000. Free radical pathways in CNS injury. J Neurotrauma 17:871-890.

Li C, Xie M, Luo F, He C, Wang J, Tan G, Hu Z. 2014. The extremely low-frequency magnetic field exposure differently affects the AMPAR and NMDAR subunit expressions in the hippocampus, entorhinal cortex and prefrontal cortex without effects on the rat spatial learning and memory. Environ Res 134:74-80.

Losi G, Garzon G, Puia G. 2008. Nongenomic regulation of glutamatergic neurotransmission in hippocampus by thyroid hormones. Neuroscience 151:155-163.

Madjid Ansari A, Farzampour S, Sadr A, Shekarchi B, Majidzadeh-A K. 2016. Effects of short term and long term extremely low frequency magnetic field on depressive disorder in mice: Involvement of nitric oxide pathway. Life Sci 146:52-57.

Mahdavi SM, Sahraei H, Yaghmaei P, Tavakoli H. 2014. Effects of electromagnetic radiation exposure on stress-related behaviors and stress hormones in male Wistar rats. Biomol Ther (Seoul) 22:570-576.

Manojlović-Stojanoski M, Nestorović N, Ristić N, Trifunović S, Ajdžanović V, Šošić-Jurjević B, Milošević V. 2012. Pregnancy reduces the responsiveness of the pituitary-adrenal axis to dexamethasone. Acta Histochem 114:562-570.

Manojlović-Stojanoski M, Nestorović N, Trifunović S, Ristić N, Jarić I, Filipović B, Milošević V. 2016. Dexamethasone exposure affects paraventricular nucleus and pituitary corticotrophs in female rat fetuses: An unbiased stereological and immunohistochemical study. Tissue Cell 48:516-523.

Matavulj M, Rajkovic V, Uscebrika G, Zikic D, Stevanovic D, Lazetic B. 1999. Electromagnetic field effects on the morphology of rat thyroid gland. In Bersani F (ed): Electricity and Magnetism in Biology and Medicine. New York, NY: Kluwer Academic/Plenum Publishers, pp 489-492.

Mendes-de-Aguiar CB, Alchini R, Decker H, Alvarez-Silva M, Tasca CI, Trentin AG. 2008. Thyroid hormone increases astrocytic glutamate uptake and protects astrocytes and neurons against glutamate toxicity. J Neurosci Res 86:3117-3125.

Murdoch J, Hall R. 1990. Brain protection: physiological and pharmacological considerations. Part I: The physiology of brain injury. Can J Anaesth 37:663-671.

O'Keefe LM, Conway SE, Czap A, Malchoff CD, Benashski S, Fortunato G, Staff I, McCullough LD. 2015. Thyroid hormones and functional outcomes after ischemic stroke. Thyroid Res 8:9.

Radak D, Resanovic I, Isenovic ER3. 2014. Changes in hypothalamus-pituitary-adrenal axis following transient ischemic attack. Angiology 65:723-732.

Rajkovic V, Matavulj M, Gledic D, Lazetic B. 2003. Evaluation of rat thyroid gland morphophysiological status after three months exposure to 50 Hz electromagnetic field. Tissue Cell 35:223-231.

Rajkovic V, Matavulj M, Johansson O. 2006. Light and electron microscopic study of the thyroid gland in rats exposed to power-frequency electromagnetic fields. J Exp Biol 209:3322-3328.

Rauš Balind S, Manojlović-Stojanoski M, Milošević V, Todorović D, Nikolić L, Petković B. 2016. Short- and long-term exposure to alternating magnetic field (50 Hz, 0.5 mT) affects rat pituitary ACTH cells: Stereological study. Environ Toxicol 31:461-468.

Rauš Balind S, Selaković V, Radenović L, Prolić Z, Janać B. 2014. Extremely low frequency magnetic field (50 Hz, 0.5 mT) reduces oxidative stress in the brain of gerbils submitted to global cerebral ischemia. PLoS One 9:e88921.

Rauš S, Selaković V, Manojlović-Stojanoski M, Radenović L, Prolić Z, Janać B. 2013. Response of hippocampal neurons and glial cells to alternating magnetic field in gerbils submitted to global cerebral ischemia. Neurotox Res 23:79-91.

Rauš S, Selaković V, Radenović L, Prolić Z, Janać B. 2012. Extremely low frequency magnetic field induced changes in motor behaviour of gerbils submitted to global cerebral ischemia. Behav Brain Res 228:241-246.

Selaković V, Rauš Balind S, Radenović L, Prolić Z, Janać B. 2013. Age-dependent effects of ELF-MF on oxidative stress in the brain of Mongolian gerbils. Cell Biochem Biophys 66:513-521.

Selmaoui B, Lambrozo J, Touitou Y. 1997. Endocrine functions in young men exposed for one night to a 50-Hz magnetic field. A circadian study of pituitary, thyroid and adrenocortical hormones. Life Sci 61:473-486.

Sert C, Akdag MZ, Çelik MS, Dasdag S. 1999. Effects of whole body chronic 50 Hz sinusoidal weak magnetic field exposure on the rat pituitary hormones. Biochem Arch 15:311-315.

Smith SM, Vale WW. 2006. The role of the hypothalamic-pituitary-adrenal axis in neuroendocrine responses to stress. Dialogues Clin Neurosci 8:383-395.

Suda S, Muraga K, Kanamaru T, Okubo S, Abe A, Aoki J, Suzuki K, Sakamoto Y, Shimoyama T, Nito C, Kimura K. 2016. Low free triiodothyronine predicts poor functional outcome after acute ischemic stroke. J Neurol Sci 368:89-93.

Szemerszky R, Zelena D, Barna I, Bárdos G. 2010. Stress-related endocrinological and psychopathological effects of short- and long-term 50Hz electromagnetic field exposure in rats. Brain Res Bull 81:92-99.

Touitou Y, Selmaoui B. 2012. The effects of extremely low-frequency magnetic fields on melatonin and cortisol, two marker rhythms of the circadian system. Dialogues Clin Neurosci 14:381-399.

Uchoa ET, Aguilera G, Herman JP, Fiedler JL, Deak T, de Sousa MB. 2014. Novel aspects of hypothalamic-pituitary-adrenal axis regulation and glucocorticoid actions. J Neuroendocrinol 26: 557-572.

WHO. 1984. Extremely Low Frequency (ELF) Fields. Environmental Health Criteria Report 35. Geneva (CH): World Health Organization.

Zanchi NE. 2010. Glucocorticoids: Extensive physiological actions modulated through multiple mechanisms of gene regulation. J Cell Physiol 224:311-315.

Zhang J, Huang J, Aximujiang K, Xu C, Ahemaiti A, Wu G, Zhong L, Yunusi K. 2018. Thyroid Dysfunction, Neurological disorder and immunosuppression as the consequences of long-term combined stress. Sci Rep 8:4552.

FIGURE LEGENDS

Fig. 1. Photograph (A) and schematic overview (B) of the system for ELF magnetic field exposure, as well as 3D plots indicating the magnetic field values measured in the horizontal plane on the bottom (z = -9 cm), in the middle (z = 0, gray marked rectangle), and on the top (z = 9 cm) of the cage (C). The center of the cage represents the null point. 1 – electromagnet; 2 – animal cage; 3 – magnetic force lines.

Fig. 2. Anterior pituitary volume. Each bar represents the mean ± SEM (n = 5-6 animals/group). The dashed line shows the control value (0.63 ± 0.02).

Fig. 3. Representative micrographs of immunohistochemically labeled ACTH cells (A-G) and the volume density of ACTH cells (H) in the anterior pituitary *pars distalis*. Control group (A), ELF-MF group immediately (B) and 7 days after cessation of exposure (C), Ischemia group on the 7^{th} (D) and 14^{th} reperfusion day (E), Ischemia + ELF-MF group on the 7^{th} day (F) and 14^{th} day after onset of the experiment (G). The scale bar represents 40 μm. The volume density of ACTH cells is presented as the mean ± SEM (n = 5-6 animals/group). The dashed line shows the control value (19.13 ± 1.26). *$p<0.05$ and ***$p<0.001$ compared to the control value; $^{###}p<0.001$ 7^{th} day *vs.* 14^{th} day after onset of the experiment (one-way ANOVA, LSD).

Fig. 4. Representative micrographs of immunofluorescence labeled ACTH cells (A-G) and RIF of ACTH cells (H) in the anterior pituitary *pars distalis*. Control group (A), ELF-MF group immediately (B) and 7 days after cessation of exposure (C), Ischemia group on the 7^{th} (D) and 14^{th} reperfusion day (E), Ischemia + ELF-MF on the 7^{th} day (F) and 14^{th} day after onset of the experiment (G). The scale bar represents 75 μm. RIF of ACTH cells is presented as the mean ± SEM (n = 5-6 animals/group). The dashed line shows the control value (0.76 ± 0.07). *$p<0.05$ compared to the control value (one-way ANOVA, LSD).

Fig. 5. Plasma ACTH concentration. Each bar represents the mean ± SEM (n = 5-6 animals/group). The dashed line shows the control value (129.76 ± 20.76). *$p<0.05$ compared to the control value; $^{#}p<0.05$ 7^{th} day *vs.* 14^{th} day after onset of the experiment (one-way ANOVA, LSD).

Fig. 6. Representative micrographs of immunohistochemically labeled TSH cells (A-G) and the volume density of TSH cells (H) in the anterior pituitary *pars distalis*. Control group (A), ELF-MF group immediately (B) and 7 days after cessation of exposure (C), Ischemia group on the 7^{th} (D) and 14^{th} reperfusion day (E), Ischemia + ELF-MF group on the 7^{th} day (F) and 14^{th} day after onset of the experiment (G). The scale bar represents 40 μm. The volume density of TSH cells is presented as the mean ± SEM (n = 5-6 animals/group). The dashed line shows the control value (4.01 ± 0.71).

Fig. 7. Representative micrographs of immunofluorescence labeled TSHβ cells (A-G) and RIF of TSHβ cells (H) in the anterior pituitary *pars distalis*. Control group (A), ELF-MF group immediately (B) and 7 days after cessation of exposure (C), Ischemia group on the 7^{th} (D) and 14^{th} reperfusion day (E), Ischemia + ELF-MF on the 7^{th} day (F) and 14^{th} day after onset of the experiment (G). The scale bar represents 250 μm. RIF of TSHβ cells is presented as the mean ± SEM (n = 5-6 animals/group). The dashed line shows the control value (0.65 ± 0.08). *$p<0.05$ and **$p<0.01$ compared to the control value; $^{\#}p<0.05$ 7^{th} day *vs.* 14^{th} day after onset of the experiment (one-way ANOVA, LSD).

Fig. 8. Serum TSH concentration. Each bar represents the mean ± SEM (n = 5-6 animals/group). The dashed line shows the control value (0.46 ± 0.07). *$p<0.05$ and **$p<0.01$ compared to the control value; $^{\#}p<0.05$ and $^{\#\#}p<0.01$ 7^{th} day *vs.* 14^{th} day after onset of the experiment (one-way ANOVA, LSD).

A

B

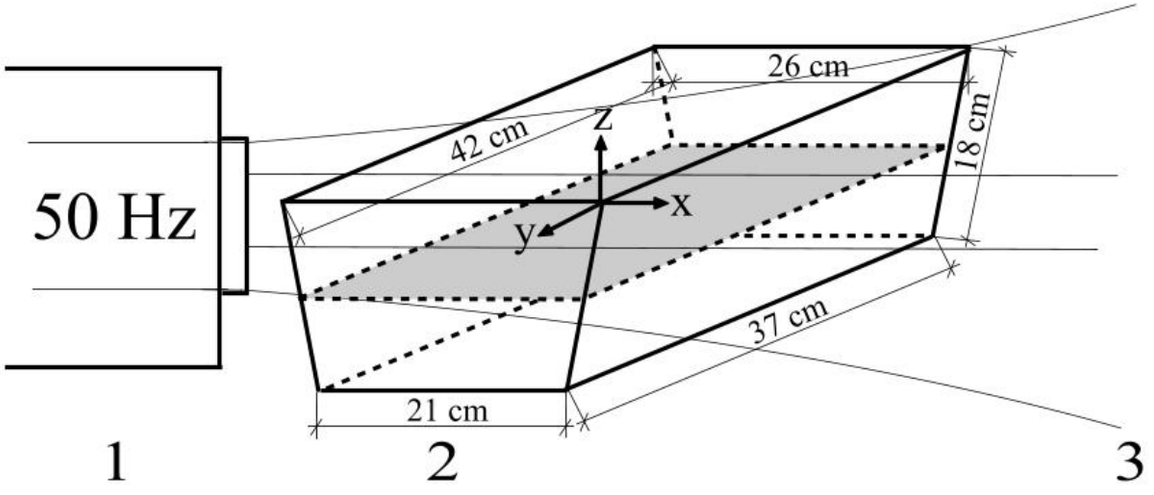
50 Hz
26 cm
42 cm
18 cm
z
x
y
37 cm
21 cm
1
2
3

C

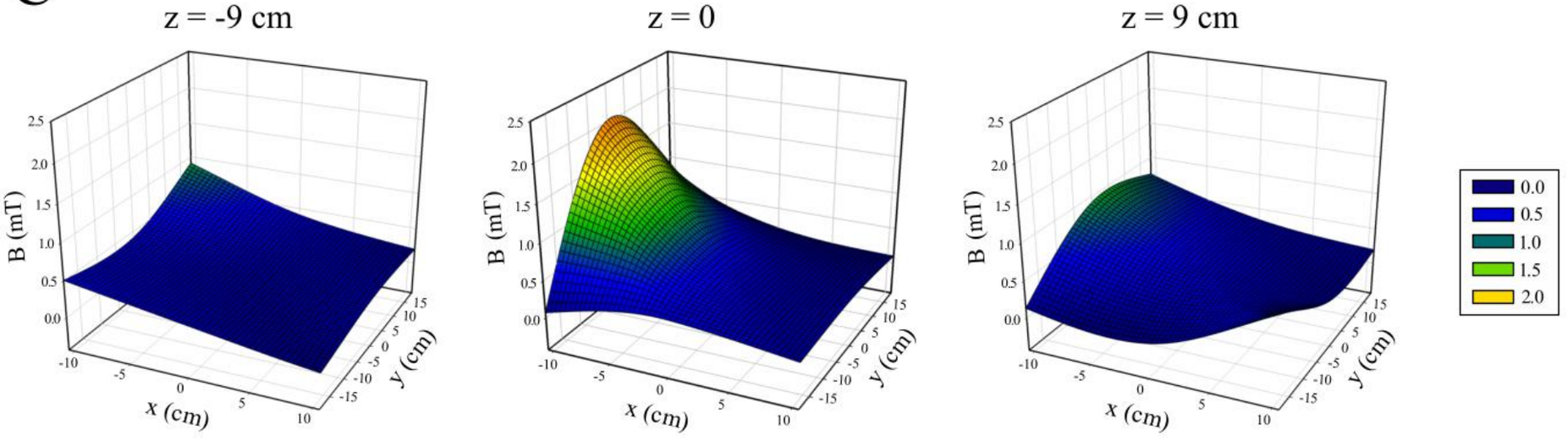
z = -9 cm
z = 0
z = 9 cm
B (mT)
x (cm)
y (cm)
0.0
0.5
1.0
1.5
2.0

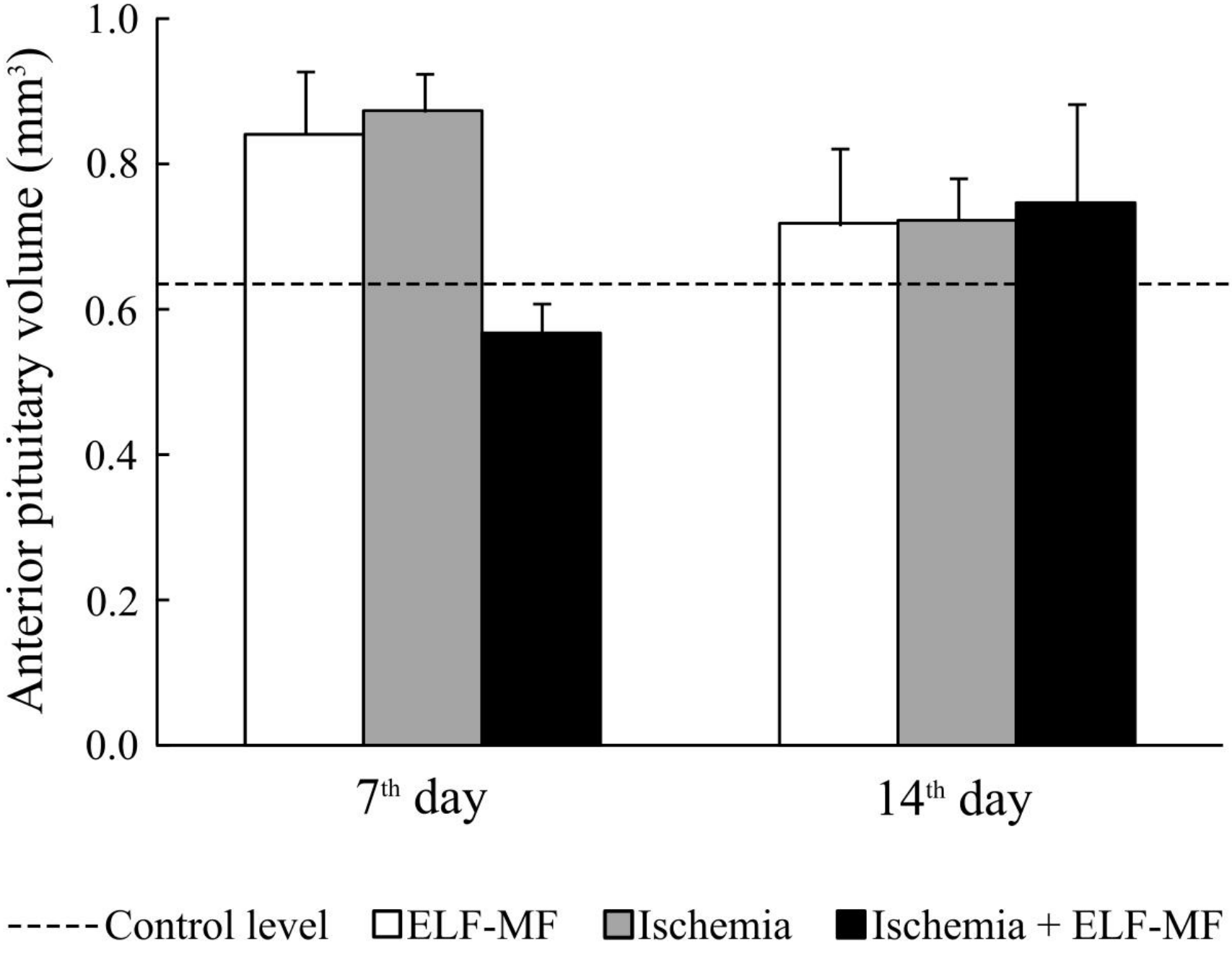
Anterior pituitary volume (mm³)
1.0
0.8
0.6
0.4
0.2
0.0
7th day
14th day
Control level
ELF-MF
Ischemia
Ischemia + ELF-MF

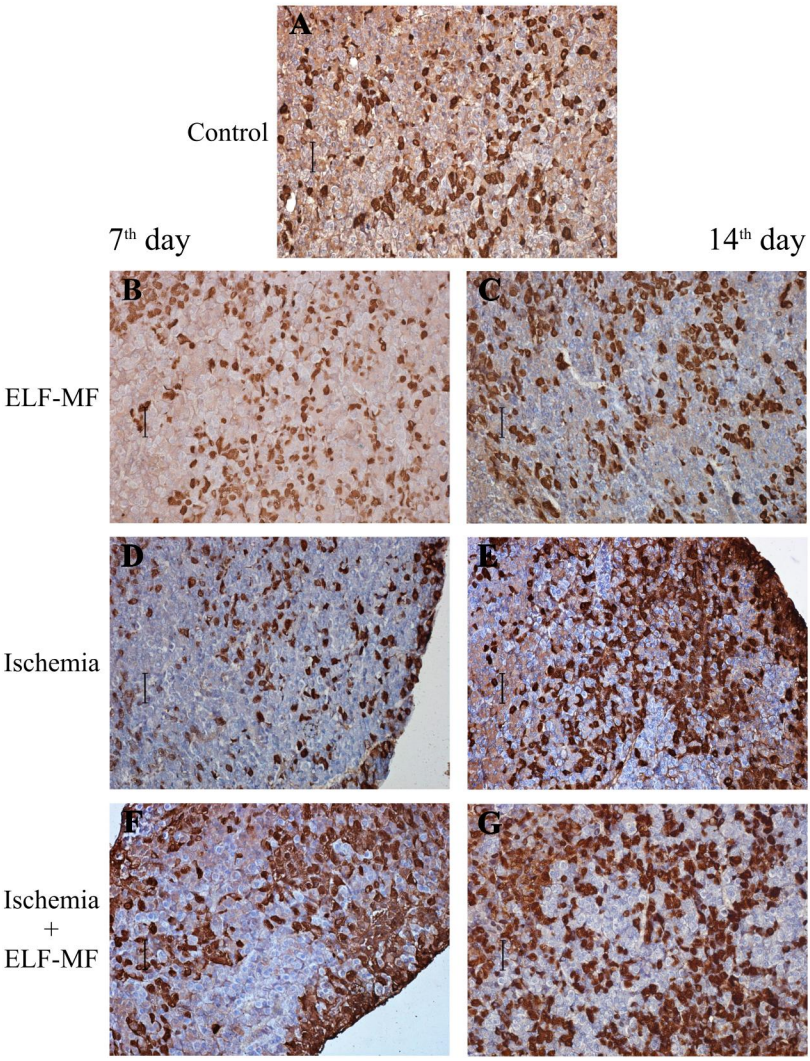
A
Control
7th day
14th day
B
C
ELF-MF
D
E
Ischemia
F
G
Ischemia
+
ELF-MF

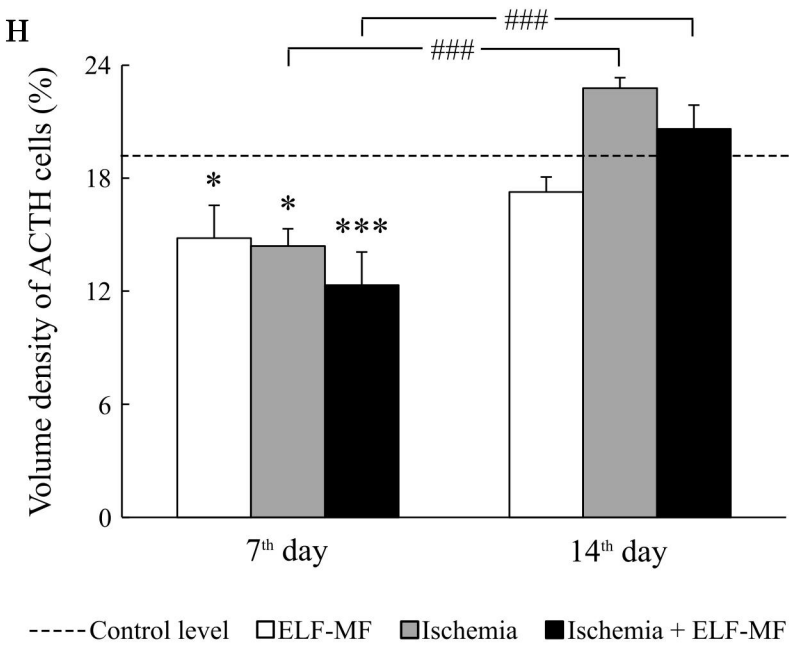
H
###
###
24
18
12
6
0
Volume density of ACTH cells (%)
*
*
***
7th day
14th day
Control level
ELF-MF
Ischemia
Ischemia + ELF-MF

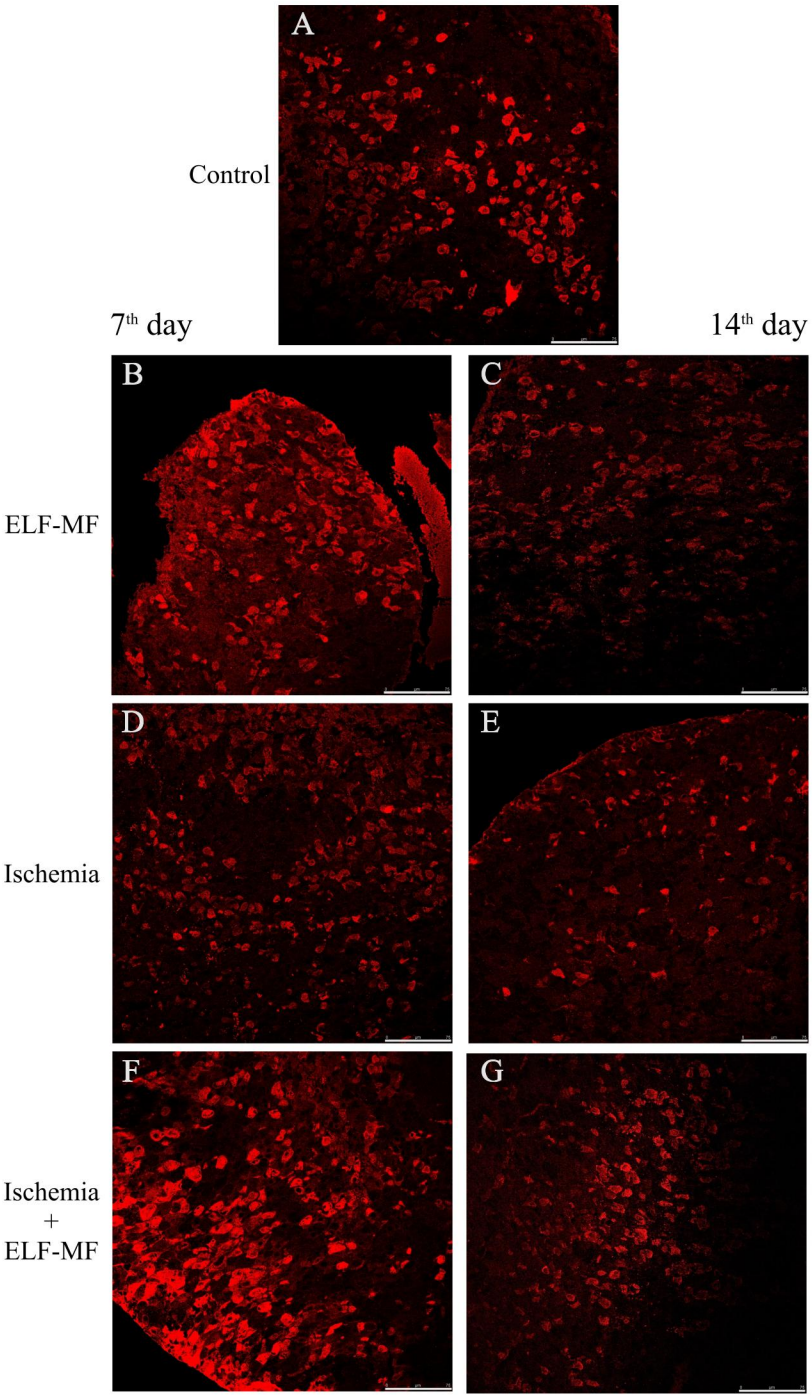
A
Control
7th day
14th day
B
C
ELF-MF
D
E
Ischemia
F
G
Ischemia
+
ELF-MF

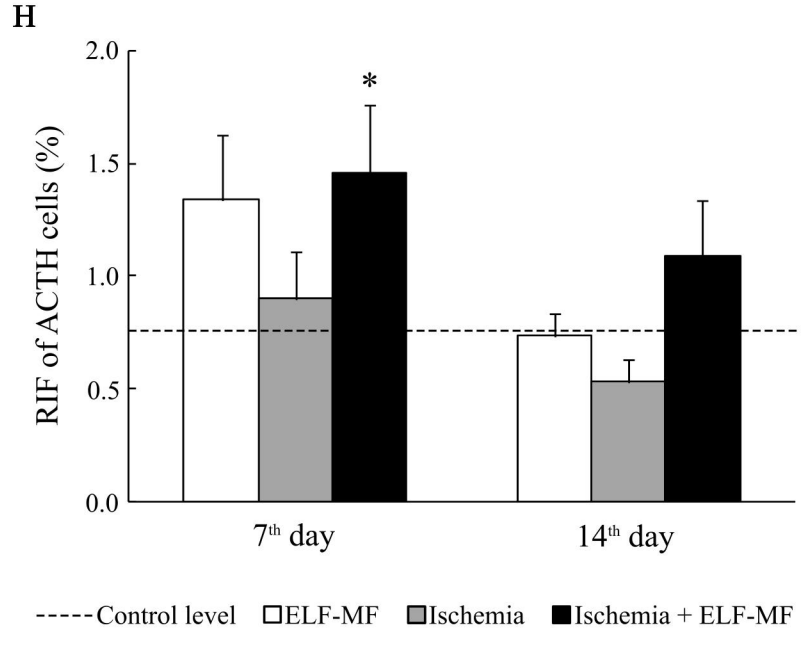
H
2.0
1.5
1.0
0.5
0.0
RIF of ACTH cells (%)
*
7th day
14th day
Control level
ELF-MF
Ischemia
Ischemia + ELF-MF

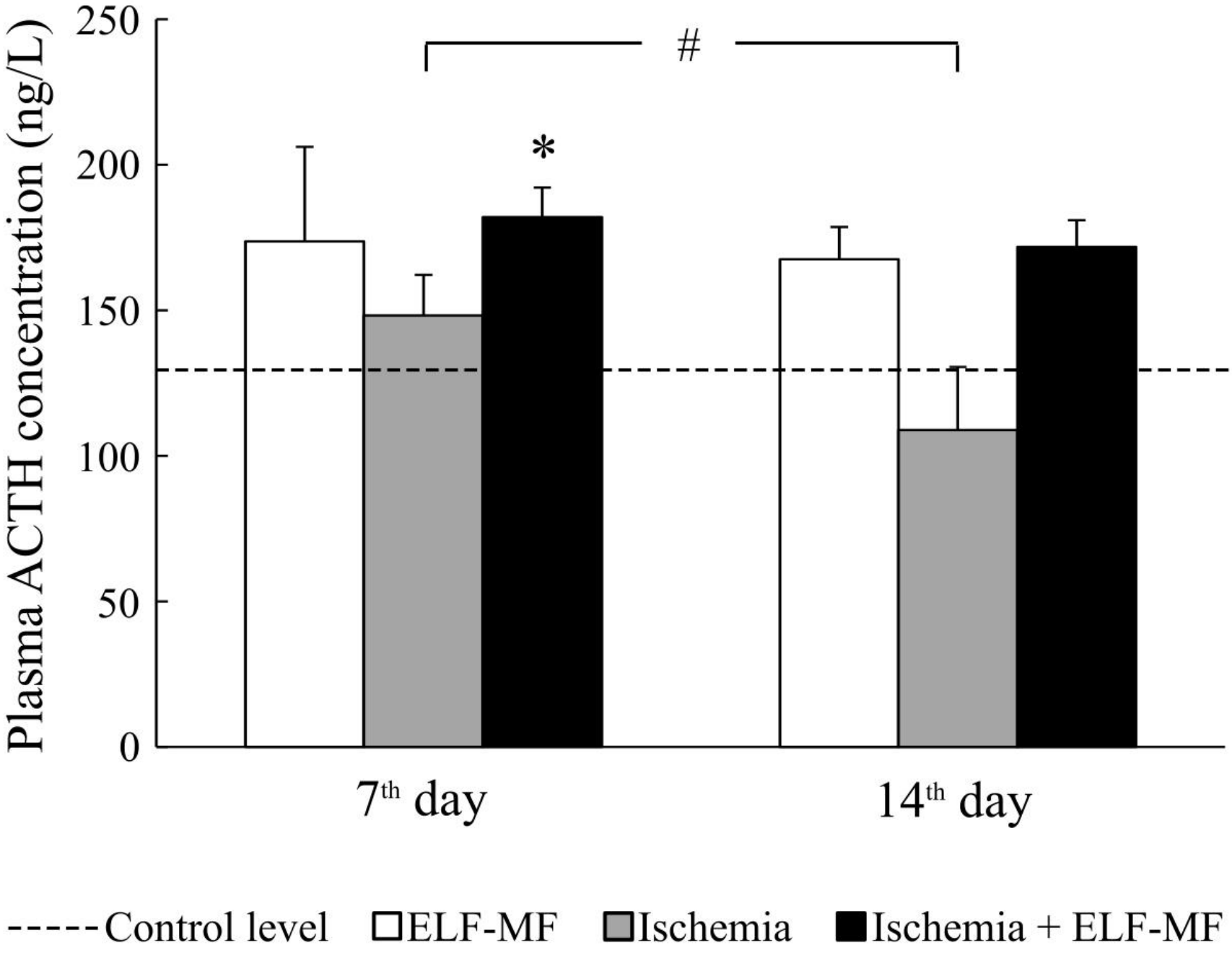
Plasma ACTH concentration (ng/L)
250
200
150
100
50
0
#
*
7th day
14th day
Control level
ELF-MF
Ischemia
Ischemia + ELF-MF

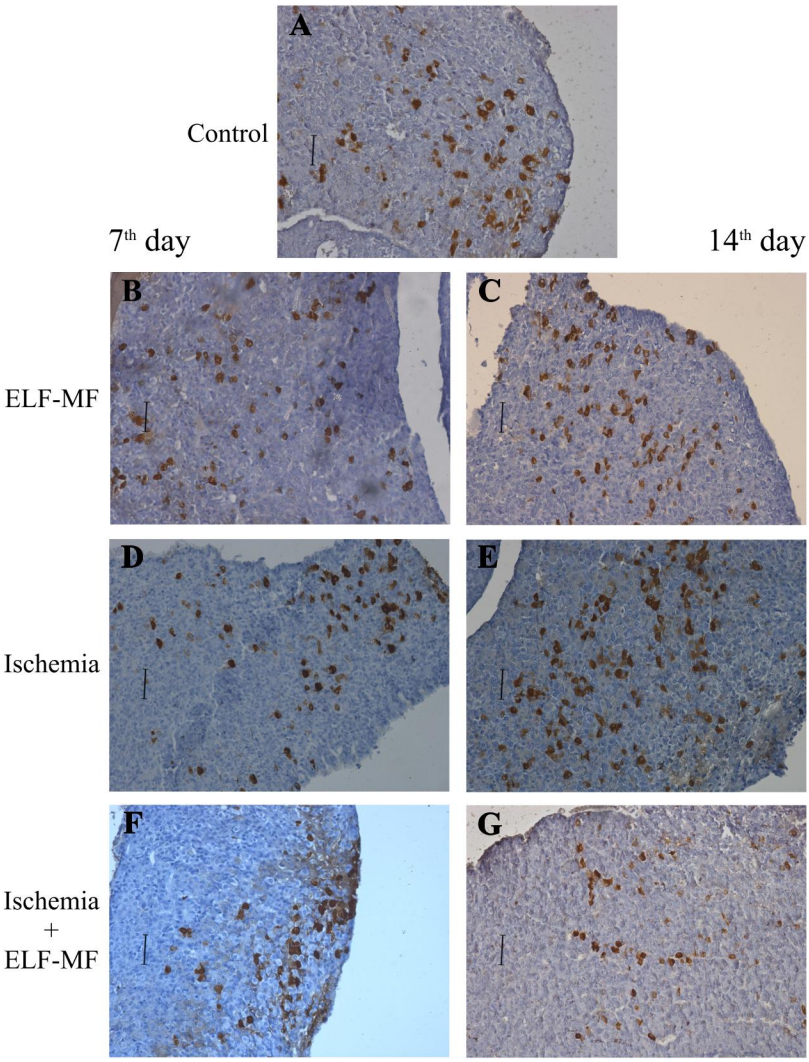
A
Control
7th day
14th day
B
C
ELF-MF
D
E
Ischemia
F
G
Ischemia
+
ELF-MF

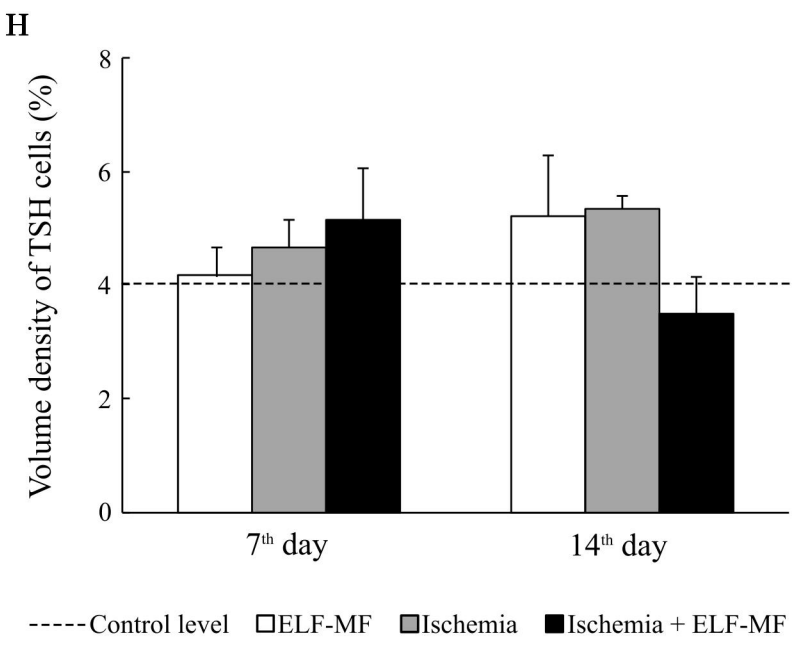
H
Volume density of TSH cells (%)
8
6
4
2
0
7th day
14th day
Control level
ELF-MF
Ischemia
Ischemia + ELF-MF

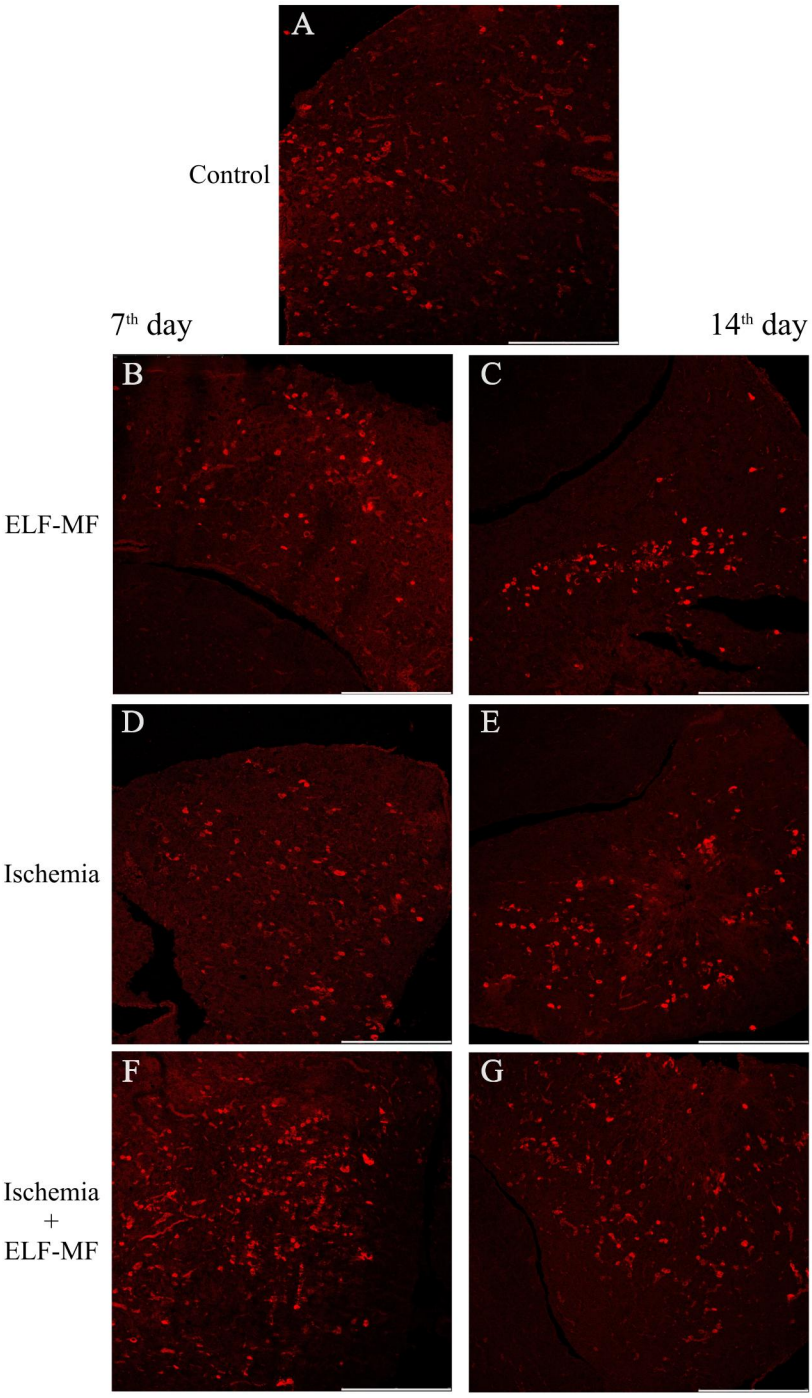
A
Control
7th day
14th day
B
C
ELF-MF
D
E
Ischemia
F
G
Ischemia
+
ELF-MF

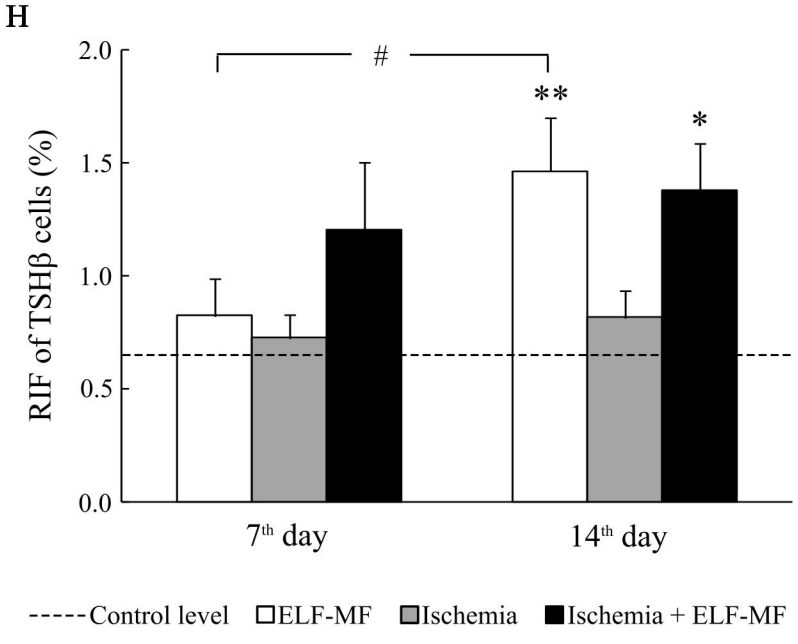
H
2.0
1.5
1.0
0.5
0.0
RIF of TSHβ cells (%)
#
**
*
7th day
14th day
Control level
ELF-MF
Ischemia
Ischemia + ELF-MF

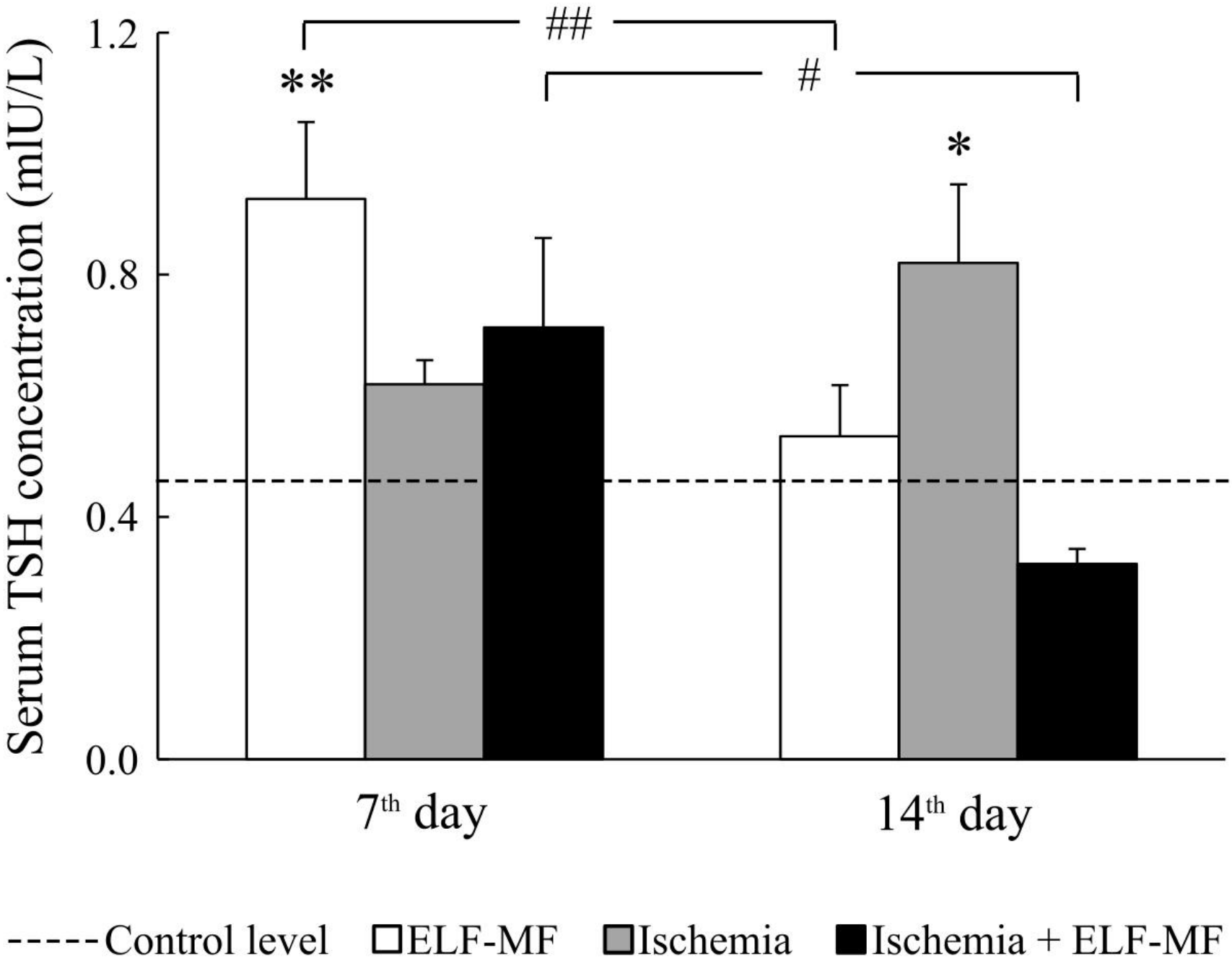
Serum TSH concentration (mIU/L)
1.2
0.8
0.4
0.0
##
#
**
*
7th day
14th day
Control level
ELF-MF
Ischemia
Ischemia + ELF-MF